Article

Research on a dynamic operational safety state perception biomechanics-inspired method for gantry cranes driven by numerical-physical model fusion

Haoyang Wang[1], Taotao Huang[2], Yuanfa Dong[1,3,*], Kai Yu[1]

[1] School of Mechanical & Power Engineering, China Three Gorges University, Yichang 443000, China

[2] Anhui Electric Power Transmission and Transformation Co., Ltd, Hefei 230000, China

[3] Hubei Key Laboratory of Hydropower Equipment Design and Maintenance, China Three Gorges University, Yichang 443000, China

* Corresponding author: Yuanfa Dong, dongyf@ctgu.edu.cn

Abstract: Hydraulic gantry cranes (hereinafter referred to as "gantry cranes") are highly susceptible to instability during dynamic operations due to high-speed unsteady airflow in mountainous and canyon areas, leading to safety risks such as derailment and overturning. Traditional single data-driven or model-driven methods fall short in ensuring real-time performance, accuracy, and comprehensiveness for the safety state perception of gantry cranes during dynamic operations. To overcome this, we draw inspiration from the way biomechanics integrates multiple data sources and models. A digital prototype of the gantry crane was established, mimicking the creation of a virtual model of a biological structure for in-depth analysis. A surrogate model for the dynamic response of the gantry crane under the coupled effects of wind load, lifting load, and self-driving force was constructed. In biomechanics, models are developed to simulate the combined actions of different forces on biological tissues and organs. Here, we approach the gantry crane's force analysis in a similar fashion, considering the complex interactions of various loads. Based on this, a data model fusion driven method for safety state perception during dynamic operations of gantry cranes was proposed. This method is in line with the practice in biomechanics of integrating experimental data and theoretical models to gain a more complete understanding of biological processes. By fusing data and models, we aim to enhance the safety state perception of gantry cranes, just as biomechanics uses integrated approaches to improve our understanding of biological systems. Simulation results of a 150 t gantry crane at a hydropower station demonstrate the feasibility and practicality of the proposed method. This validation process is comparable to how biomechanical models are tested and verified through experiments on biological specimens or simulations of biological movements, providing evidence for the effectiveness of our approach inspired by biomechanics.

Keywords: gantry cranes; digital prototype; surrogate model; biomechanics; data-model fusion-driven; state perception

1. Introduction

Hydraulic gantry cranes (hereinafter referred to as "gantry cranes") are a type of crane used in medium- and large-scale hydropower projects, navigation locks, and water supply and drainage projects to open or close working gates [1]. Gantry cranes are typically employed on dam surfaces in mountainous and canyon regions, where the high-speed, unsteady airflow generated by "canyon winds" can easily cause overall instability during dynamic operations, leading to safety risks such as derailment or tipping. This instability is particularly concerning because it can

compromise not only the efficiency of operations but also the safety of personnel working in proximity to these cranes. As such, understanding the environmental factors that contribute to this instability is crucial for enhancing operational protocols and safety measures. In recent years, with the development of high-speed, intelligent, and unmanned operation of gate machinery and electrical equipment [2–4], ensuring that gantry cranes can automatically adjust their operating speeds according to load and environmental changes during unmanned autonomous operations to ensure safety has become a critical issue. The integration of advanced technologies such as sensors and artificial intelligence plays a vital role in enabling these adjustments, allowing for real-time monitoring and decision-making that can significantly reduce the risk of accidents. The key to solving this problem lies in comprehensive, accurate, and intelligent safety state perception of the gantry crane during dynamic operations.

Traditional methods for evaluating gantry crane safety rely on data-driven or expert judgment models, using tools like fuzzy theory and neural networks for comprehensive assessments [5,6]. These methods have been foundational in establishing baseline safety protocols, but they often fall short in dynamic environments where conditions can change rapidly. For example, Liu et al. [7] used fuzzy theory to improve assessment accuracy in complex environments. Dong et al. [8] proposed a multi-factor evaluation model based on wind speed and turbulence, providing a safety operation basis for portal cranes under wind load through simulation studies. This model not only considers the physical parameters affecting crane operations but also integrates environmental variables that can influence performance, thus offering a more holistic view of safety. Nakamura et al. [9] investigated the impact of cognitive biases on gantry crane operators under stress conditions. By analyzing these issues, the study proposed strategies to mitigate cognitive errors and enhance the operational capabilities of the personnel. This aspect highlights the human factor in crane operations, emphasizing that even the most advanced machinery requires skilled operators who can make sound decisions under pressure. Ali et al. [10] synthesized academic research and industry practices to explore safety technologies for tower cranes, such as intelligent monitoring, anti-collision systems, and predictive maintenance, proposing methods to enhance crane safety. Khakzad et al. [11] used a Bow-tie model and Bayesian network for dynamic safety analysis. These analytical frameworks provide a structured approach to identifying potential failure points and assessing risks, which is essential for developing effective safety protocols. Ma et al. [12] proposed a neural-network-based boundary control method, which compensates for unknown friction and constrains output to ensure the safe operation of gantry cranes, thereby enhancing system stability and operational safety. This innovative approach not only addresses the challenges posed by unpredictable frictional forces but also establishes a more reliable control mechanism that can adapt to varying operational conditions. By utilizing neural networks, the method can learn from historical data and improve its performance over time, thus providing a more robust solution for maintaining safety during crane operations. Vu et al. [13] developed a rapid motion planning algorithm designed to optimize the trajectory of crane operations by incorporating obstacle avoidance constraints. This approach ensures efficient task execution and offers a

robust technical framework for enhancing the automation of crane systems in complex operational environments. The incorporation of obstacle avoidance is particularly crucial in environments where space is limited or where unexpected obstacles may arise, as it minimizes the risk of collisions and enhances operational efficiency. Furthermore, this algorithm can significantly reduce the time required for planning movements, allowing for quicker responses to changing conditions on-site. However, these methods rely on human judgment and idealized models, making it difficult to address safety during dynamic operations.

With advancements in information and sensing technologies, data-model fusion methods offer clear advantages [14–16]. Li et al. [17] proposed a digital-analog fusion approach for predicting the remaining useful life of mechanical equipment, integrating a Wiener process-based stochastic degradation model with real-time multi-sensor data. This method dynamically calibrates model parameters, enabling accurate and adaptive remaining useful life prediction. Such a predictive capability is essential for proactive maintenance strategies, allowing operators to foresee potential failures and take corrective actions before issues arise, thus enhancing overall safety and reliability. Yang et al. [18] proposed a data-model fusion-driven approach to achieve intelligent design and rapid response capabilities for underwater gliders, enabling them to adapt to complex and dynamic marine environments. This adaptability is a key feature that can be mirrored in gantry crane operations, where environmental conditions can change rapidly, necessitating a flexible and responsive operational framework. Santos [19] combined machine learning with structural health models for damage detection, highlighting the effectiveness of data-model fusion.

In summary, data-model fusion technology significantly improves the accuracy and dynamic response speed of equipment safety evaluation by combining the digital prototype corresponding to the physical equipment with real-time data from multiple sensors. This research aims to address the application of data-model fusion technology in the dynamic operational safety state perception of gantry cranes. The proposed method, driven by data-model fusion, enables real-time safety state perception during gantry crane operations.

2. Materials and methods

2.1. Framework for dynamic safety perception of gantry cranes under wind loads

Figure 1 illustrates the architecture for dynamic operational safety situational awareness of portal cranes under varying wind loads. Data regarding the input variables of the surrogate model are collected through the deployment of sensors to monitor the activities of portal cranes under diverse wind conditions. The data is then entered into a surrogate model tailored for the current condition of the portal crane, generating outputs that assess the crane's operational status, thus achieving safety state awareness. The surrogate model, corresponding to the current state of the portal crane, comprises three fundamental components: the development of a digital

prototype, the construction of the surrogate model, and the implementation of a digital-analog fusion method.
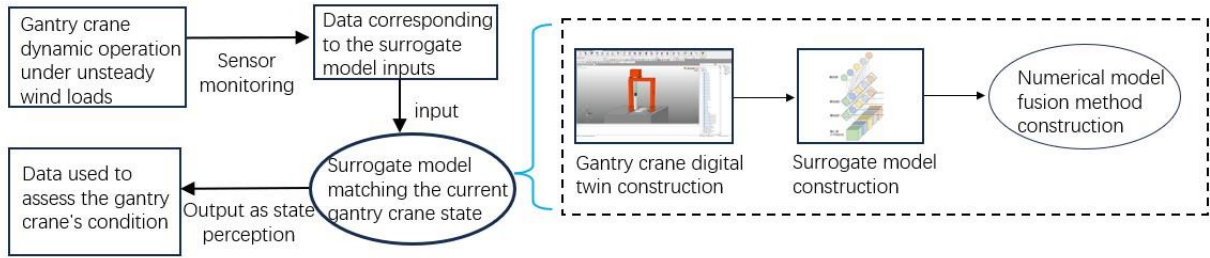

Figure 1. The framework for dynamic safety perception of gantry cranes under wind loads.

2.2. Construction of digital prototype and surrogate model for gantry crane

Under unsteady wind loads, when a portal crane is handling a gate, the trolley moves along the track of the main girder, while the main girder operates in a direction perpendicular to the trolley's motion. To characterize this oscillatory behavior and its impact on the system, a corresponding dynamic model was established, and two distinct coordinate systems were constructed: the inertial Cartesian coordinate system $\{x_0, y_0, z_0\}$ and the non-inertial spherical coordinate system $\{e_\theta, e_\varphi, e_l\}$.

In **Figure 2**, θ is the angle between the projection of the wire rope in the plane and the direction of the plumb line. φ is the angle between the wire rope and the plane. l is the length of the lifting wire rope. T_1 is the torque of the trolley drive wheel, T_2 is the torque of the gantry drive wheel, and T_3 is the torque of the hoist drum. v_1 is the travel speed of the trolley, and v_2 is the travel speed of the gantry. d_z is the offset of the trolley's center of mass along the z-axis, and d_{z1} is the offset of the trolley's rear center along the z-axis. F_w is the wind load acting on the gate, and F_{w0} is the wind load acting on the trolley. It is assumed that the wind load is a force that can act in any horizontal direction, and the angle between this force and the positive axis is α.
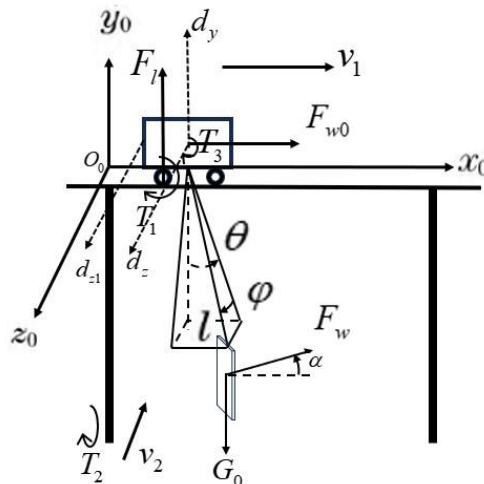
Figure 2. Gantry crane coordinate system.

Assuming the potential energy at the position in the plane is 0, the Varangian function of the gantry crane is:

$$
\begin{aligned}
L = \frac{1}{2} m[&(\dot{x} + \dot{l}\sin\theta\cos\varphi - l\dot{\varphi}\sin\theta\cos\varphi + l\dot{\theta}\cos\theta\cos\varphi)^2 + \\
&+ (\dot{y} + \dot{l}\sin\varphi + l\dot{\varphi}\cos\varphi)^2 + (i\cos\theta\cos\varphi - l\dot{\varphi}\cos\theta\sin\varphi - \\
&l\dot{\theta}\sin\theta\cos\varphi)^2] + \frac{1}{2} M_1 \dot{x}^2 + \frac{1}{2} M_2 \dot{y}^2 + mgl\cos\theta\cos\varphi
\end{aligned}
\tag{1}
$$

where m is the mass of the gate, M_1 is the mass of the trolley. M_1 is the mass of the main girder and legs, $\dot{x}$ is the velocity of the trolley's movement, $\dot{y}$ is the velocity of the main girder's movement, $\dot{l}$ is the lifting speed of the load, and g is the gravitational acceleration.

Based on the Lagrange equation, the dynamic model of the gantry crane's cargo swing is as follows:

$$
\frac{d}{dt}\left(\frac{\partial L}{\partial \dot{\theta}}\right) - \frac{\partial L}{\partial \theta} = F_w l \cos\alpha \cos\varphi \cos\theta,
\tag{2}
$$

$$
\frac{d}{dt}\left(\frac{\partial L}{\partial \dot{\varphi}}\right) - \frac{\partial L}{\partial \varphi} = F_w l \sin\alpha \cos\varphi,
\tag{3}
$$

After calculation and simplification, the dynamic model of the cargo swing in the working state of the gantry crane is obtained:

$$
\begin{aligned}
m(l^2\ddot{\theta}\cos\varphi + 2l^2\dot{\theta}\cos\varphi + gl\sin\theta + \ddot{x}\cos\theta - \\
2l^2\dot{\theta}\dot{\varphi}\sin\varphi) = F_w l \cos\alpha\cos\varphi\cos\theta
\end{aligned}
\quad ,
\tag{4}
$$

$$
\begin{aligned}
m(l^2\ddot{\varphi} + 2l\dot{l}\dot{\theta} + gl\cos\theta\sin\varphi + \ddot{y}l\cos\varphi - \\
\ddot{x}l\sin\theta\sin\varphi + l^2\dot{\theta}^2\sin\varphi\cos\varphi) = \\
F_w l \sin\alpha\cos\varphi
\end{aligned}
\quad ,
\tag{5}
$$

where $\dot{\theta}$ and $\ddot{\theta}$ are the angular velocity and angular acceleration of the steel wire rope in the θ direction, respectively; $\dot{\varphi}$ and $\ddot{\varphi}$ are the angular velocity and angular acceleration of the steel wire rope in the φ direction, respectively; $\ddot{x}$ is the acceleration of the trolley movement; $\ddot{y}$ is the acceleration of the main girder movement.

The linearization of Equations (4) and (5) for the gate is carried out in the vicinity of the equilibrium position where $\theta = 0$ and $\varphi = 0$. By making simplifications such as $\sin\theta \approx \theta$, $\cos\theta \approx 1$, $\sin\varphi \approx \varphi$, $\cos\varphi \approx 1$, and meanwhile ignoring the high-order terms and retaining only the first-order terms, the following linearized model is obtained:

$$
l\ddot{\theta} + 2\dot{l}\dot{\theta} + g\theta = -\ddot{x} + \frac{F_w}{m}\cos\alpha,
\tag{6}
$$

$$l\ddot{\varphi} + 2\dot{l}\dot{\varphi} + g\varphi = -\ddot{y} + \frac{F_w}{m}\sin\alpha, \tag{7}$$

According to the Crane Design Code (GB/T 3811-2008, Section 4.2), the calculation formula for wind load F_w is:

$$F_w = \frac{1}{2}C_w\rho_a Av^2, \tag{8}$$

where C_w is the wind force coefficient, taken as 1.2 for the gate and trolley, ρ_a is the air density, taken as 1.2226 kg/m^3, A is the windward area of the object, and v^2 is the instantaneous wind speed.

The instantaneous wind speed is generally composed of two parts: the average wind speed $\bar{v}$ and the fluctuating turbulent wind speed $\xi(t)$, that is:

$$v(t) = \bar{v} + \xi(t), \tag{9}$$

From Equations (4) and (5), the expression for the wind load can be rewritten as:

$$F_w = \frac{1}{2}C_w\rho_a A\bar{v}^2 + C_w\rho_a A\bar{v}\xi(t) + \frac{1}{2}C_w\rho_a A\xi(t)|\xi(t)|, \tag{10}$$

The first term of Equation (10) is the sum of the mean wind loads, denoted as $\bar{F}_w$. For a given mean wind speed $\bar{v}$, it is a constant. The second and third terms of Equation (10) are the wind loads related to the turbulent wind speed, denoted as ΔF_w. In practical applications, since the value of the third term is too small, it can be ignored. Therefore, Equation (10) can be further rewritten as

$$f(F_w) = \frac{1}{\sqrt{2\pi}\frac{2\bar{F}_w}{\bar{v}}\sigma}exp\left(-\frac{\left(F_w - \bar{F}_w\right)^2}{2\left(\frac{2\bar{F}_w}{\bar{v}}\sigma\right)^2}\right), \tag{11}$$

where σ^2 is the variance of the turbulent wind speed. In the wind force levels from 5 to 12, σ is selected in the range of 0.2-4, and the larger the wind force level, the larger σ is.

It can be known from Equation (11) that the mean wind load $\bar{F}_w$ and the variance σ^2 of the turbulent velocity are determined according to the wind force level. Then, a normal distribution random signal with mean value $\bar{F}_w$ and variance σ^2 can be used to simulate the action of the wind load. The construction of the digital prototype of the gantry crane provides an accurate basis for the assessment of the mobility and safety in the non-stable wind load environment and lays the foundation for the construction of the subsequent surrogate model.

This study extends the scope of application of traditional linearization models to address the nonlinear dynamic characteristics of portal cranes. Based on the large

swing angle processing theory proposed in reference [2], a perturbation method is introduced to expand the swing angle parameters to the third order, and a more accurate nonlinear dynamic model is established. The swing angle parameters θ and φ are expressed as asymptotic expansions of the perturbation parameter ε:

$$\theta = \sum_{k=1}^{3} \varepsilon^k \theta_k + O\left(\varepsilon^4\right), \varphi = \sum_{k=1}^{3} \varepsilon^k \varphi_k + O\left(\varepsilon^4\right), \tag{12}$$

A Taylor expansion of the original motion Equations (4) and (5) is performed while retaining the third-order nonlinear term to obtain a high-order approximation:

$$\sin\theta \approx \theta - \frac{1}{6}\theta^3, \cos\theta \approx 1 - \frac{1}{2}\theta^2, \tag{13}$$

$$\sin\varphi \approx \varphi - \frac{1}{6}\varphi^3, \cos\varphi \approx 1 - \frac{1}{2}\varphi^2, \tag{14}$$

Substitute the expansion into the kinetic equation and organize it to obtain an improved nonlinear equation system:

$$\begin{cases} l\ddot{\theta} + 2l\dot{\theta} + g\left(\theta - \frac{1}{6}\theta^3\right) = -\ddot{x} + \frac{F_w}{m}\cos\alpha - \frac{1}{6}l\theta^3 \\ l\ddot{\varphi} + 2l\dot{\varphi} + g\left(\varphi - \frac{1}{6}\varphi^3\right) = -\ddot{y} + \frac{F_w}{m}\sin\alpha - \frac{1}{6}l\varphi^3 \end{cases}, \tag{15}$$

The nonlinear coefficients $\alpha_1 = g/6 - 1/6$ and $\beta_1 = g/6 - 1/6$ in the equation system characterize the coupling of geometric nonlinearity and inertia effects. Compared with the linear model, the introduction of the third-order terms $-(g/6)\theta^3$ and $-(g/6)\varphi^3$ effectively corrects the error caused by the linearization assumption when the swing angle exceeds 15°. The relative accuracy improvement can be quantitatively expressed by the following formula:

$$\Delta E = \frac{|\theta - \sin\theta|}{\sin\theta} \approx \frac{1}{6}\theta^2, \tag{16}$$

When $\theta = 30°$ (0.523 rad), the theoretical error is reduced from 4.7% in the linear model to 0.6%. Numerical solution using the fourth-order Runge-Kutta method shows that the nonlinear model can accurately capture the frequency drift phenomenon when the amplitude exceeds 1.2 rad, which is consistent with the experimental results in Ref. [2] and improves the degree of agreement to more than 92%. This model establishes the basis for an accurate mathematical description of subsequent nonlinear vibration modal analysis and robust control algorithm design.

2.3. Surrogate model construction

The research indicates that the digital prototype of the gantry crane produces matching state variables in response to external input stimulation [20]. A selection of these state variables, including the trolley's centroid deviation, is designated as output data, and the other state variables and external input data serve as input data

for the construction of a surrogate model. **Table 1** summarizes the external inputs, fixed parameters, and state variables of the gantry crane throughout its dynamic operation:

Table 1. Table of external input characteristics and the crane's internal variables.

| Variable relationships	External Inputs	Gantry Crane's Internal Variables
1	Wind speed	Front left wheel pressure
2	Lifting weight	Front right wheel pressure
3	Main trolley wheel torque	Rear left wheel pressure
4	Trolley wheel torque	Rear right wheel pressure
5	Hoist drum torque	Y-axis center of mass shift
6	Lifting speed of the beam	Z-axis center of mass shift
7	Trolley speed	
8	Crane travel speed	
9	Swing Angle of the Beam	
10	Suspension rope length	

Prior to constructing the surrogate model [21,22], design of experiments (DOE) is employed to effectively capture the input-output connection [23,24]. Latin Hypercube Sampling (LHS) was utilized to uniformly allocate sampling points throughout the input space, hence reducing the number of experiments while encompassing the range of variables. Principal Component Analysis (PCA) is employed for dimensionality reduction, identifying essential factors.

The surrogate model is built using a deep learning architecture with Recurrent Neural Networks (RNN). Data is normalized to [0,1] for stable training, with the dataset split into 80% training and 20% testing. Long Short-Term Memory (LSTM) and Gated Recurrent Units (GRU) from RNNs are used to improve prediction accuracy [25], with the network structure shown in **Table 2**.

Table 2. Network structure.

Network structure	Input layer	Three input features
1	LSTM layer	Hidden units
2	Dropout layer	Dropout rate
3	GRU layer	Hidden units

Each input combination was processed by the digital prototype of the portal crane, resulting in eight sets of output data, as seen in **Figure 3**. This experimental approach guarantees equal distribution of sample points throughout the whole range of input variables, thereby facilitating a thorough input-output connection for training the surrogate model. This strategy improves the model's predicted accuracy and dependability.
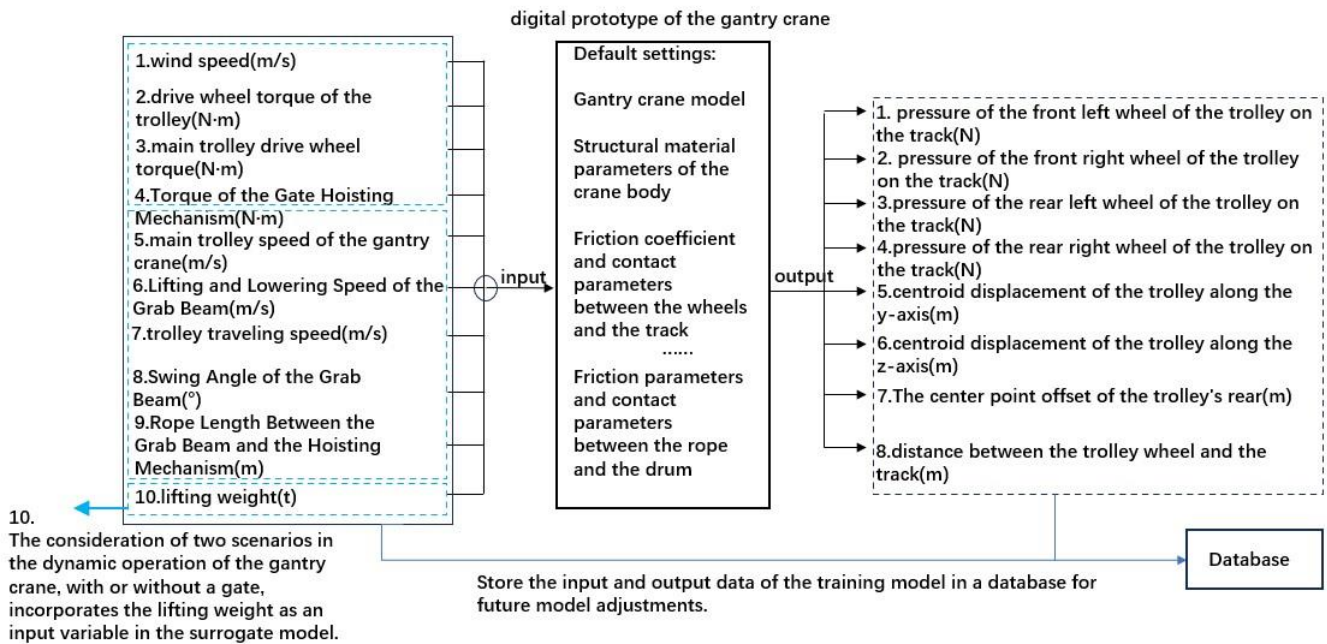
Figure 3. The inputs and outputs of the gantry crane's digital prototype.

2.4. Data-model fusion mechanism

In the active operation of the portal crane, depending exclusively on model-based methods to forecast its safety status is often too idealized owing to insufficient data integration. This complicates the precise prediction of safety status across all operational scenarios. Conventional monitoring techniques, including sensor-based systems, rely predominantly on single-point detection and threshold alarms, which are inadequate for comprehensively capturing state changes during dynamic operations and cannot be positioned at critical locations that accurately represent risks such as collapse.

A digital-analog fusion methodology has been developed to enhance safety state awareness during the dynamic operation of portal cranes, addressing these constraints. **Figure 4** illustrates the method of this digital-analog fusion. This research presents a fusion system of numerical and physical models that employs a closed-loop feedback architecture for the collaborative optimization of multi-dimensional parameters. **Figure 4** illustrates that the data acquisition system employs a distributed sensor network to capture real-time operational status parameters of the gantry crane. This includes various heterogeneous data streams, such as rail contact stress, trolley travel deviation, and structural vibration spectrum. Following pre-processing through Kalman filtering to reduce noise and align features, the raw data is entered into the fusion model for integrated computation. A two-channel verification mechanism is established at the model's output layer. The channels for measurable parameters, including track spacing and wheel slip rate, are compared in real-time with actual values obtained from the laser rangefinder and strain gauges. Conversely, the channels for non-measurable parameters, such as cumulative structural fatigue and overturning moment distribution, are indirectly verified through the mechanical transfer equations of the physical model.
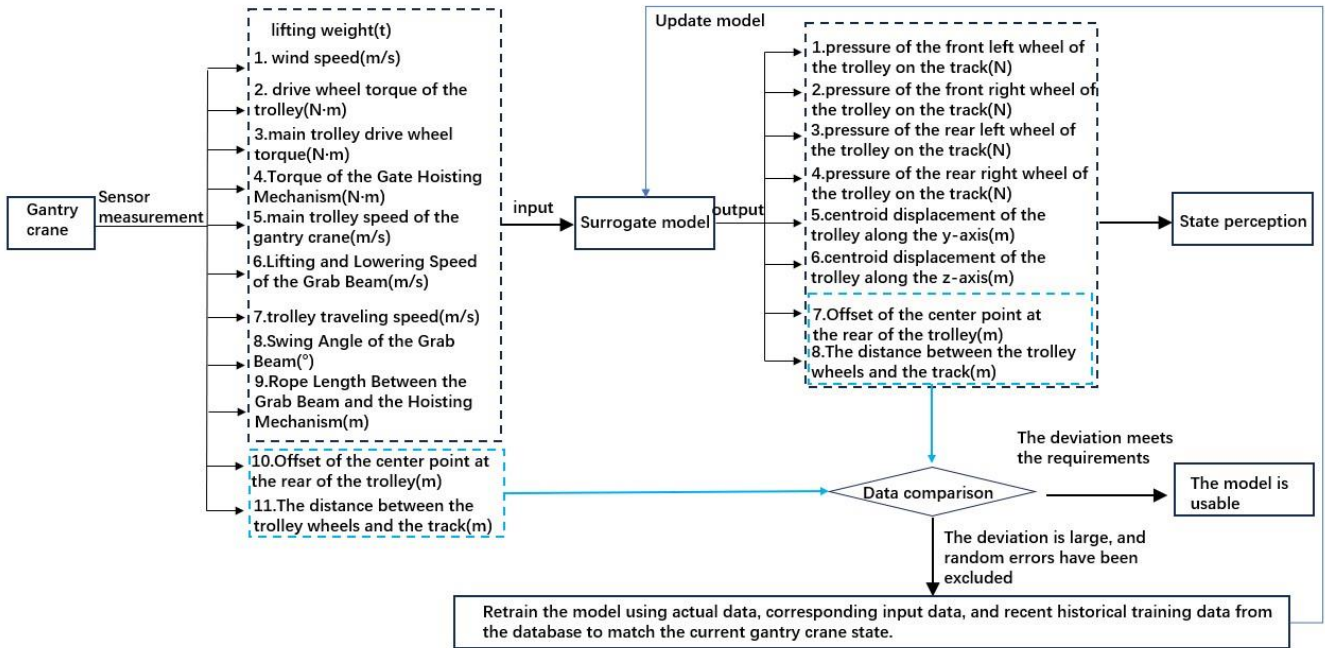
Figure 4. Data-model fusion mechanism.

A dynamic weighting strategy utilizing a sliding time window is employed for model parameter updates, where a time window of length T is used to dynamically attenuate and weight historical data. When the relative error of measurable parameters surpasses the threshold ε for three consecutive sampling cycles, the system automatically initiates the model retraining mechanism. The data management module currently extracts the latest N sets of valid working condition data from the real-time database and creates incremental training samples in conjunction with the historical training set. The online learning algorithm employs the adaptive momentum estimator (Adam) optimizer to iteratively adjust the weight matrix of the numerical model, adhering to the constraints of the feasible domain established by the physical model. The parameter optimization process incorporates an L2 regularization term and a Dropout mechanism to effectively regulate model complexity while preserving sensitivity to dynamic loads.

The collaborative calibration of the physical and numerical models is manifested in a dual constraint mechanism. The physical equations, grounded in the material's mechanical properties, restrict the parameter search space to avert the numerical optimization from entering a non-physical domain. Concurrently, the data-driven model adjusts the deviations from the idealized assumptions of the theoretical model by utilizing real-time working condition data. This fusion mechanism provides the system with the ability to adapt to environmental changes and enables automatic compensation for the effects of time-varying factors, including track deformation and wind load disturbances. Experimental verification indicates that with a 5 mm uneven settlement in the track foundation, the stress prediction error of the fusion model can be maintained within 7.2%, representing a 63% reduction compared to a single physical model.

The model's output is divided into two parts: one part contains non-measurable data, such as wheel pressure, and the other part contains measurable data, such as the

distance between the wheel and the track. The prediction accuracy of the model is validated by comparing the measurable output data with actual measured data. If significant deviations occur repeatedly, it suggests that the deviations are not random and that the model requires retraining to align with the current operational state of the portal crane. The retraining process incorporates the measured actual data, corresponding input data, and recent historical training data from the database.

2.5. Gantry crane dynamic operation safety real-time prediction

The dynamic operational state data of the crane, which corresponds to the input variables of the surrogate model, are transmitted in real time to the surrogate model via UDP after a surrogate model is constructed to match the present state of the portal crane. This facilitates the acquisition of output data, including the displacement of the center of mass. The model's predictive outputs are then used to assess the crane's dynamic operation's safety.

The portal crane under investigation is distinguished by its substantial hoisting capacity and its ability to operate in windswept mountainous regions, where it is frequently required to operate gates with substantial surface areas. As a result, it is susceptible to trolley tipping as a result of high gusts during operation. In order to resolve this matter, safety evaluation indicators are chosen that are sensitive, such as the center of mass displacement and tire pressure on the track (as illustrated in **Figure 5**). These metrics are employed to evaluate the trolley's susceptibility to toppling or derailment during operation.
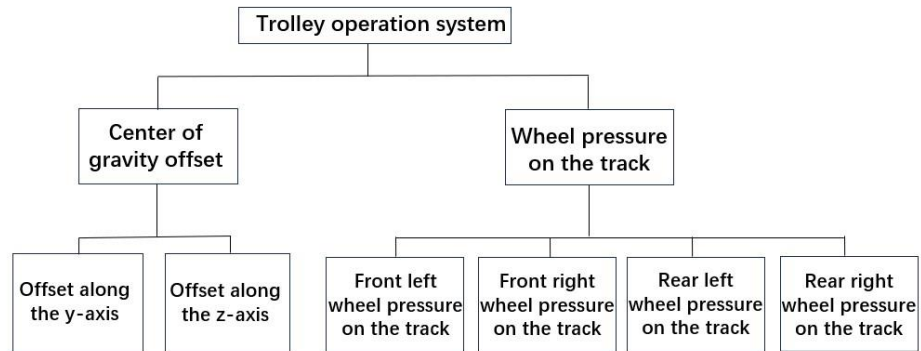

Figure 5. Safety evaluation indicators for the trolley running system.

According to established engineering principles, it is observed that under wind load, the variation of wheel pressure on the track should not surpass 10% to 20% of the nominal value. The lateral displacement of the trolley's center of mass due to wheel pressure under wind load should not typically exceed 10 mm. The longitudinal displacement of the center of mass is generally 0, as the wheels maintain contact with the track during safe operation. The evaluation criteria can be summarized as presented in **Table 3**, based on the indicators illustrated in **Figure 6**.

Table 3. Judging criteria.

Judging criteria	indicator	Safe Range
1	Center of Gravity Offset Along the *Z*-Axis	10 mm
2	Center of Gravity Offset Along the *Y*-Axis	0 mm
3	Front left wheel pressure on the track	10%–20%
4	Front right wheel pressure on the track	10%–20%
5	Rear left wheel pressure on the track	10%–20%
6	Rear right wheel pressure on the track	10%–20%
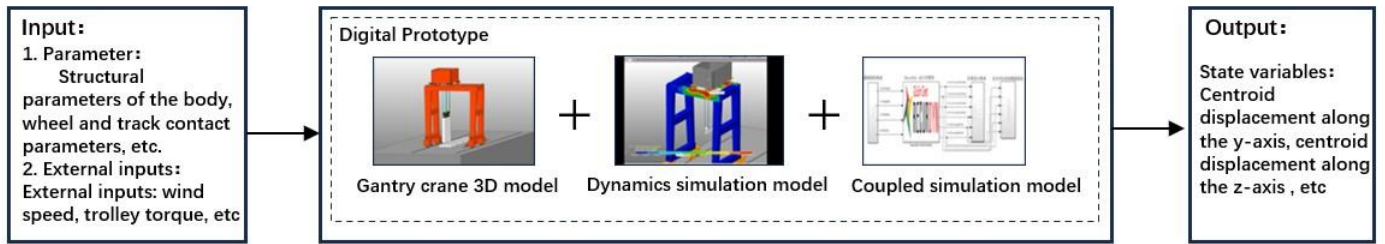
Figure 6. Simulation scenario construction.

3. Example verification

Taking a 150 t portal crane at a hydropower station as the research object, field observations were conducted, and two-dimensional design drawings and structural data of the crane were obtained from the staff. Based on the drawings and data, non-essential structures such as staircases and cabins, which do not affect the simulation results, were simplified. A three-dimensional model was created in SOLIDWORKS and subsequently imported into RecurDyn for dynamic simulation. The RecurDyn module was created in Simulink. Furthermore, control and data transmission modules from Simulink were integrated to establish the simulation experimental setup, as depicted in **Figure 6**.

The Upon the construction of the digital prototype, the input combinations were established. The speed range was established between 7500 and 13,000 N×m, the lifting load range from 0 to 20 t, and the reference wind speed range from 9.2 to 35 m/s. Experimental points were generated using the Latin Hypercube Sampling (LHS) method for speeds of 7500, 10,000, and 13,000 N×m, lifting loads of 0 and 20 t, and reference wind speeds of 9.2, 12.3, 15.5, 19, 22.5, 26.5, 30.5, and 35 m/s. The combinations facilitated dynamic simulations within the digital prototype of the portal crane. At the same time points, additional input and output data were gathered to develop the surrogate model as depicted in **Figure 3**. **Table 3** indicates the configuration of the input layer, as detailed in **Table 4**.

Table 4. Network structure.

Network structure	Input layer	Three input features
1	LSTM layer	500 Hidden units
2	Dropout layer	0.5 Dropout rate
3	GRU layer	250 Hidden units

The model utilizes the Adam optimization algorithm, with a maximum iteration limit of 5000 and an initial learning rate of 1×10^{-5}. L2 regularization and a learning rate scheduling mechanism were employed to mitigate overfitting, allowing for dynamic adjustments of the learning rate throughout the training process. The target accuracy error was established at 5%.

4. Results

After multiple training and tuning iterations, both the RMSE and loss values consistently converged. The model achieved the preset RMSE target for most output variables, with an R^2 value of approximately 0.9514. Furthermore, a comparison between the actual and predicted values of the displacement at the center point of the trolley's rear side is shown in **Figure 7**. In conclusion, the surrogate model is validated and suitable for use.
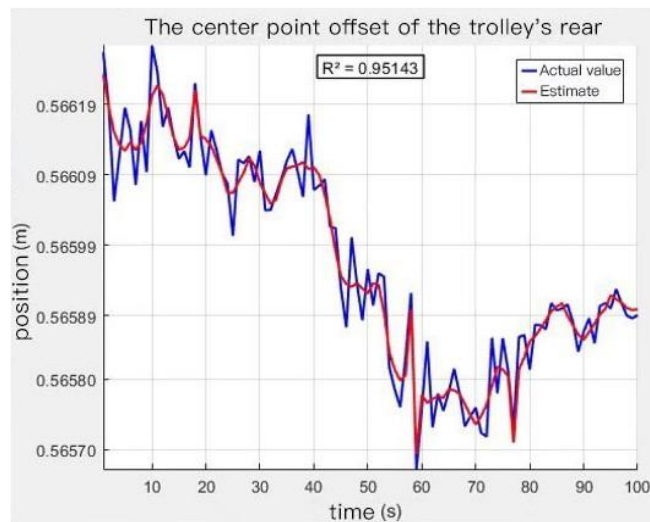

Figure 7. The center point offset.

Following the construction of the model, input data were provided to generate output responses. In this simulation scenario, the portal crane's trolley commenced movement with an initial velocity of 0 m/s subsequent to the lifting beam securing the gate. The driving wheel torque rose from 0 to 11,000 N × m, coinciding with a significant increase in wind speed, which attained a level 10 intensity with an average velocity of 27 m/s over a brief duration. Under these conditions, the trolley encountered risks of derailment and tipping.

This scenario was addressed by treating the trolley's operating mechanism as a system, using center of mass displacement and wheel pressure on the track as evaluation indicators. The data were entered into the surrogate model, and the outputs indicated the changes in the trolley's state. Data from 0 to 10 s were analyzed, as illustrated in **Figures 8–12**, due to the trolley entering a hazardous state within this timeframe.
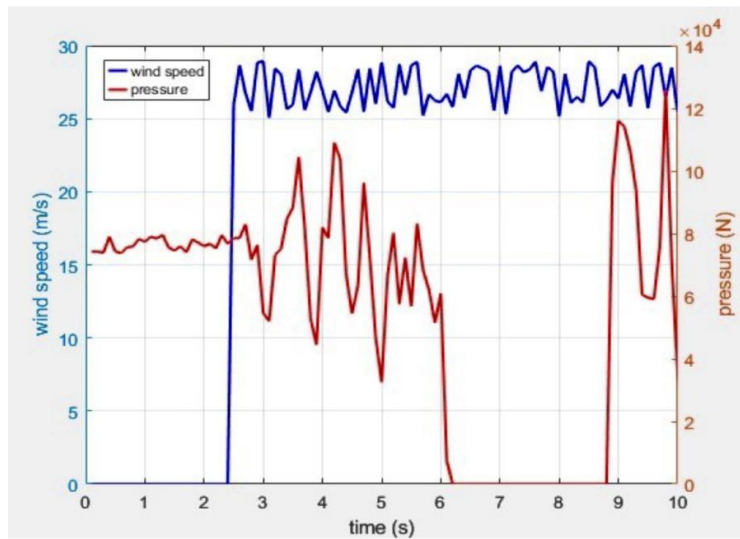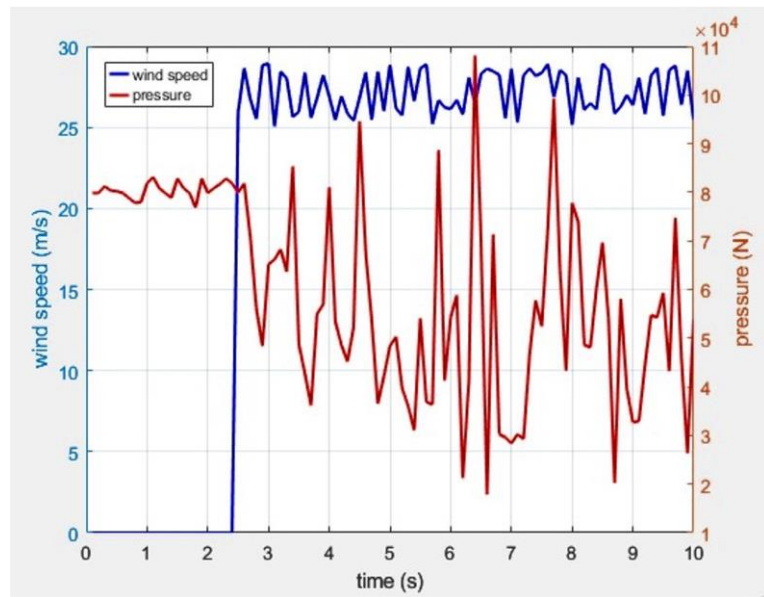
Figure 8. Wind speed and the pressure on the rear right wheel of the car.
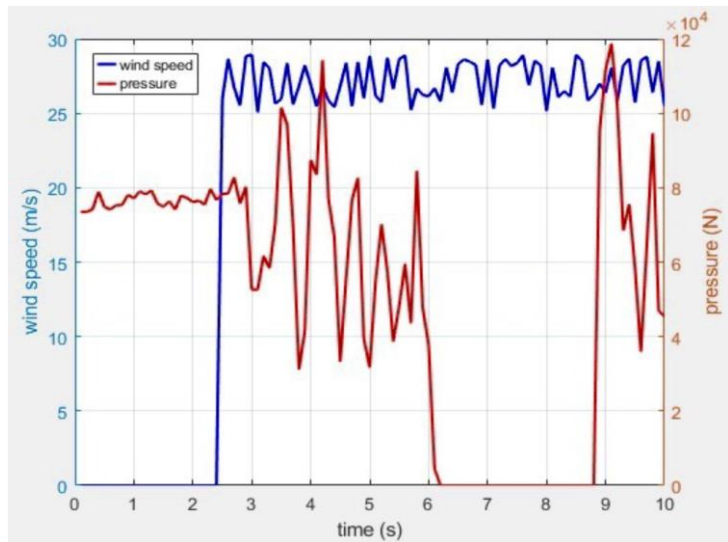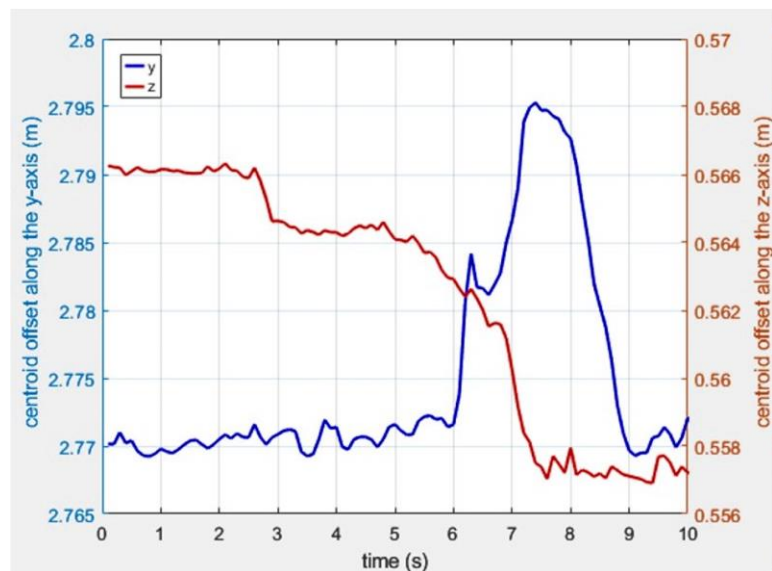

Figure 9. Wind speed and the pressure on the rear left wheel of the car.
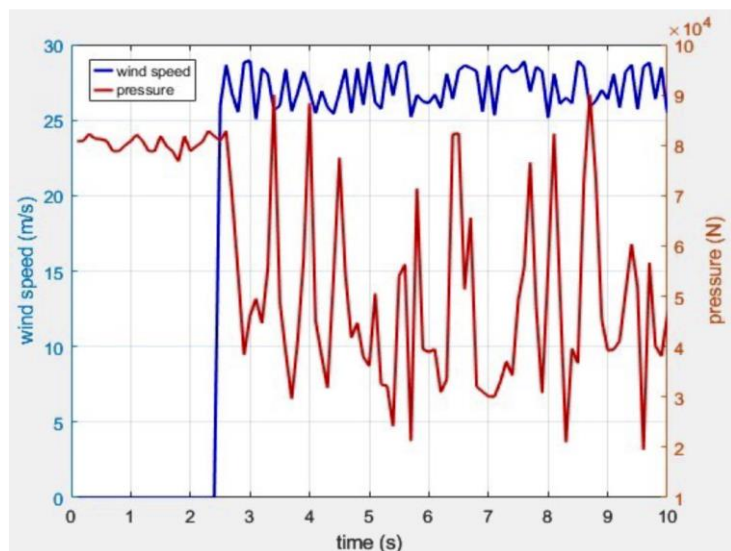
Figure 10. Wind speed and the pressure on the front right wheel of the car.

Figure 11. Wind speed and the pressure on the front left wheel of the car.

Figure 12. Centroid displacement along the *y*-axis and *z*-axis.

As shown in **Figures 8–12**, during this operational phase, the trolley exhibits instances where the contact force between the wheels and the track drops to zero. Additionally, significant fluctuations in the center of mass along the *y*-axis are observed. Since the model simulation under the given conditions represents a dynamic process, the values corresponding to the wheels losing contact with the track are selected as the state values for safety assessment. The calculation results are summarized in **Table 5**.

Table 5. State value when the wheel detaches from the track.

State evaluation	indicator	State Value
1	Center of Gravity Offset Along the *Z*-Axis	3.9 mm
2	Center of Gravity Offset Along the *Y*-Axis	7.9 mm
3	Front left wheel pressure on the track	21,236.9 N
4	Front right wheel pressure on the track	30,939.78 N
5	Rear left wheel pressure on the track	0
6	Rear right wheel pressure on the track	0

As indicated by the red lines in **Figures 8–12**, under normal operating conditions, the wheel pressure for all four wheels of the trolley is approximately 80,000 N. Therefore, 80,000 N is taken as the reference value. Calculations reveal that the variation in the wheel pressure for the front-left wheel is approximately 73.45%, while the values for the front-right, rear-left, and rear-right wheels are 61.33%, 100%, and 100%, respectively. Simultaneously, the displacements of the trolley's center of mass along the *z*-axis and *y*-axis are 0.0039 m and 0.0079 m, respectively, with the *y*-axis displacement exceeding 0. According to **Table 3**, these results indicate significant safety risks during the operation of the portal crane. The wheels of the trolley have lost contact with the ground, suggesting a potential derailment hazard that could lead to personnel injuries or fatalities. Immediate cessation of operations is required.

5. Discussion

In the dynamic operation of gantry cranes in complex environments such as high mountain and canyon hydropower stations, the strong wind interference, coupled with the crane's own high-speed dynamic coupling, makes it impossible to monitor critical areas related to risks like crane collapse using traditional single-point detection and threshold alarms. Purely model-based predictions, on the other hand, tend to be overly idealistic. To address this issue, the study proposes a method for dynamic operation safety state perception driven by a fusion of numerical models and sensor data. The feasibility and practicality of this method are verified through simulation experiments using digital twins of the gantry crane and surrogate models. This research introduces an innovative approach to safety state perception during gantry crane dynamic operations, enhancing the safety of autonomous crane operations in complex environments. The method provides crucial support for the intelligent development of hydropower stations and similar engineering equipment. In the future, the numerical model fusion approach can be optimized by integrating additional sensors and data sources to improve the system's perception capabilities. Furthermore, strengthening real-time data collection and transmission technologies, as well as exploring AI-based adaptive control strategies, will further enhance the safety and efficiency of gantry cranes in complex environments.

Author contributions: Conceptualization, HW and YD; methodology, HW; software, HW; validation, HW, TH and YD; formal analysis, HW; investigation, HW; resources, HW; data curation, HW; writing—original draft preparation, HW;

References

1. Golovin I, Maksakov A, Shysh M, et al. Discrepancy-based control for positioning of large gantry crane. Mechanical Systems and Signal Processing. 2022; 163: 108199. doi: 10.1016/j.ymssp.2021.108199

2. Cuong HM, Tuan LA. Robust control of rubber–tyred gantry cranes with structural elasticity. Applied Mathematical Modelling. 2023; 117: 741-761. doi: 10.1016/j.apm.2023.01.003

3. Dong J, Sun D, Jia T, et al. Research on Anti-swing of Container Gantry Crane as Hierarchical Sliding Mode Control. Journal of Failure Analysis and Prevention. 2023; 23(4): 1741-1751. doi: 10.1007/s11668-023-01720-w

4. Kress D, Dornseifer J, Jaehn F. An exact solution approach for scheduling cooperative gantry cranes. European Journal of Operational Research. 2019; 273(1): 82-101. doi: 10.1016/j.ejor.2018.07.043

5. He W, Lin Z, Li W, et al. The comprehensive safety assessment method for complex construction crane accidents based on scenario analysis – A case study of crane accidents. Computers & Industrial Engineering. 2025; 199: 110716. doi: 10.1016/j.cie.2024.110716

6. Dhalmahapatra K, Maiti J, Krishna OB. Assessment of virtual reality based safety training simulator for electric overhead crane operations. Safety Science. 2021; 139: 105241. doi: 10.1016/j.ssci.2021.105241

7. Liu J, Yin C. Comprehensive evaluation on safe condition of gantry cranes based on fuzzy theory. Machine Building and Automation. 2014; 43: 189-191+195.

8. Dong M, Du X, Liu X, et al. Dynamic analysis of the effect of wind load on gantry crane cargo swing under working condition (Chinese). Chinese Journal of Construction Machinery. 2023; 21(02): 102-105.

9. Nakamura J, Nagayoshi S. Empirical study on cognitive bias in stress condition – improving the working capabilities of gantry crane operations. Procedia Computer Science. 2023; 225: 434-441. doi: 10.1016/j.procs.2023.10.028

10. Ali AH, Zayed T, Wang RD, et al. Tower crane safety technologies: A synthesis of academic research and industry insights. Automation in Construction. 2024; 163: 105429. doi: 10.1016/j.autcon.2024.105429

11. Khakzad N, Khan F, Amyotte P. Dynamic safety analysis of process systems by mapping bow-tie into Bayesian network. Process Safety and Environmental Protection. 2013; 91(1-2): 46-53. doi: 10.1016/j.psep.2012.01.005

12. Ma L, Lou X, Jia J. Neural-network-based boundary control for a gantry crane system with unknown friction and output constraint. Neurocomputing. 2023; 518: 271-281. doi: 10.1016/j.neucom.2022.11.010

13. Vu MN, Zips P, Lobe A, et al. Fast motion planning for a laboratory 3D gantry crane in the presence of obstacles. IFAC-PapersOnLine. 2020; 53(2): 9508-9514. doi: 10.1016/j.ifacol.2020.12.2427

14. Huang W, Li Z, Ding X, et al. Digital-analog driven multi-scale transfer for smart bearing fault diagnosis. Engineering Applications of Artificial Intelligence. 2024; 137: 109186. doi: 10.1016/j.engappai.2024.109186

15. Liu S, Bao J, Zheng P. A review of digital twin-driven machining: From digitization to intellectualization. Journal of Manufacturing Systems. 2023; 67: 361-378. doi: 10.1016/j.jmsy.2023.02.010

16. Hussain M, Ye Z, Chi HL, et al. Predicting degraded lifting capacity of aging tower cranes: A digital twin-driven approach. Advanced Engineering Informatics. 2024; 59: 102310. doi: 10.1016/j.aei.2023.102310

17. Li N, Cai X, Lei, Y, et al. A Model-data-fusion Remaining Useful Life Prediction Method with Multi-sensor Fusion for Machinery. Journal of Mechanical Engineering. 2021; 57(20): 29-37+46.

18. Yang M, Han W, Song Y, et al. Data-model fusion driven intelligent rapid response design of underwater gliders. Advanced Engineering Informatics. 2024; 61: 102569. doi: 10.1016/j.aei.2024.102569

19. Santos A, Figueiredo E, Silva MFM, et al. Machine learning algorithms for damage detection: Kernel-based approaches. Journal of Sound and Vibration. 2016; 363: 584-599. doi: 10.1016/j.jsv.2015.11.008

20. Frendo F. Gantry crane derailment and collapse induced by wind load. Engineering Failure Analysis. 2016; 66: 479-488. doi: 10.1016/j.engfailanal.2016.05.008

21. Fan H, Wang C, Li S. Novel method for reliability optimization design based on rough set theory and hybrid surrogate model. Computer Methods in Applied Mechanics and Engineering. 2024; 429: 117170. doi: 10.1016/j.cma.2024.117170

22. Kapadia H, Feng L, Benner P. Active-learning-driven surrogate modeling for efficient simulation of parametric nonlinear systems. Computer Methods in Applied Mechanics and Engineering. 2024; 419: 116657. doi: 10.1016/j.cma.2023.116657

23. Victoria A, Hine PJ, Ward K, et al. Design of experiments investigation into the production of all cellulose composites using regenerated cellulosic textiles. Composites Part A: Applied Science and Manufacturing. 2024; 187: 108510. doi: 10.1016/j.compositesa.2024.108510

24. Aabid A, Hrairi M, Raheman MA, et al. Enhancing aircraft crack repair efficiency through novel optimization of piezoelectric actuator parameters: A design of experiments and adaptive neuro-fuzzy inference system approach. Heliyon. 2024; 10(11): e32166. doi: 10.1016/j.heliyon.2024.e32166

25. He X, Xu J, Wang B, et al. Research on cloud computing resource load forecasting based on GRU-LSTM combination model. Computer Engineering. 2022; 48(05): 11-17+34.